Quantum cascade lasers designed toward shorter wavelengths

2016 J. Phys.: Condens. Matter 28 065302

(http://iopscience.iop.org/0953-8984/28/6/065302)

IOP Publishing Journal of Physics: Condensed Matter
J. Phys.: Condens. Matter **28** (2016) 065302 (6pp) doi:10.1088/0953-8984/28/6/065302

Quantum cascade lasers designed toward shorter wavelengths

Jilian Xu[1,2], Lei Liu[1], Bing Hui Li[1], Zhenzhong Zhang[1], Jian Ma[1], Kewei Liu[1], Jun He[3] and D Z Shen[1]

[1] State Key Laboratory of Luminescence and Applications, Changchun Institute of Optics, Fine Mechanics and Physics, Chinese Academy of Sciences, No.3888 Dongnanhu Road, Changchun 130033, People's Republic of China
[2] University of Chinese Academy of Sciences, Beijing 100049, People's Republic of China
[3] School of Physics Science and Technology, Central South University, Changsha 410083, People's Republic of China

E-mail: liulei@ciomp.ac.cn and shendz@ciomp.ac.cn

Received 27 May 2015, revised 12 August 2015
Accepted for publication 18 August 2015
Published 21 January 2016

Abstract

Quantum cascade lasers (QCLs) are normally based on one-dimensional confined quantum wells. In this scheme, it is still a challenge to produce lasing with a frequency higher than mid-infrared. Here, we discuss the possibility to extend the spectral range of QCLs to the higher frequency region by adding another dimensional confinement. Taking the ZnO/MgO system as an example, we demonstrate theoretically that such a two-dimensional confined QCL can operate at wavelengths from the near-infrared $\lambda = 2.95$ μm, 1.57 μm, 1.13 μm to the visible 734 nm.

Keywords: zinc oxide, quantum cascade laser, quantum wire

(Some figures may appear in colour only in the online journal)

1. Introduction

QCLs are semiconductor lasers that achieve lasing emission by the intersubband transitions of multiple quantum wells [1]. Normally, the spectral coverage of QCLs has been limited to the wavelength region of infrared and terahertz [2–11]. Historically, there have been many attempts of trying to make them work at the higher frequency region, but at most, they can emit mid-infrared lights. In 1998, Faist *et al* achieved the QCL lasing at about 3.4 μm, based on the strain-compensated InGaAs/AlInAs structure [12]. Eight years later, the QCLs emitting near 3.1–3.3 μm were demonstrated by Devenson *et al* based on the InAs/AlSb system [13]. In 2007, the InGaAs-based QCLs emitting at 3.05 μm [14, 15] and the InAs-based ones emitting at 2.95 μm [3] and 2.75 μm [4] were reported. In 2010, Cathabard *et al* demonstrated the InAs-based QCLs operating at 2.63–2.65 μm that is the shortest wavelength reported so far on QCLs [2].

In fact, the limitation of the spectral range of QCLs is intrinsic, since all QCLs, by now, have been built on the one-dimensional confined quantum well heterostructures. As illustrated in figure 1, the lasing emission of QCLs is determined by the energy separation ($\triangle E_{21}$) between the first (E_1) and the second exited state (E_2). Whereas, the population inversion is typically realized via the resonant longitudinal optical (LO) phonon emission from the first exited state (E_1) to the ground state (E_0). The energy difference $\triangle E_{10}$ ($=E_1–E_0$) between them is fixed to the energies of LO-phonons which are normally tens of meVs in semiconductors. Given the fact that $\triangle E_{21}$ scales almost linearly with $\triangle E_{10}$, it is difficult to increase $\triangle E_{21}$ above the mid-infrared region while still keep $\triangle E_{21}$ within tens of meVs. Nevertheless, such a dilemma can be overcome, if we confine those electrons for lasing in another dimension and thereby produce more energy levels with tunable separations. In that case the optical transition can be selected more freely for lasing than the one-dimensional confined QCLs. In 2003, Keck *et al* suggested a quantum cascade emitter structure that is based on electronic transitions in an artificial band structure of coupled quantum wires [16]. They also pointed out that the quantum wire structure analyzed could not be superior over the layered systems due to the existence of a large number of subbands in the active region of the emitter.

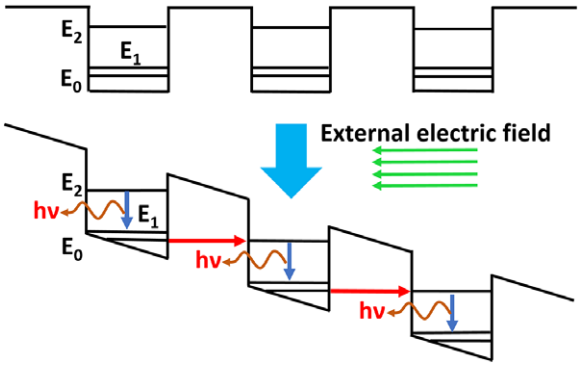

Figure 1. Schematic illustration of the photon emission process of a conventional three-level scheme QCL.

In this work, we will examine the alignment of electronic subbands and their transition rates in coupled two-dimensional confined quantum wells, and discuss the possibility of using the two-dimensional confined quantum cascade laser scheme to extend the spectral range down to shorter wavelengths. Here, the ZnO/MgO system was selected since the large band offset between ZnO and MgO [17–20] is sufficient to accomodate higher energies of intersubband transitions. Besides, the energy of the LO-phonon in ZnO is about 72 meV [21–23] which is much larger than the room-temperature thermal energy of 26 meV. That means the LO-phonon energy is high enough to prevent the turbulence of the QCLs' performance caused by the thermally activated backfilling [24–29].

2. Calculational details

The Schrödinger equations based on the effective mass approximation were solved with the finite element method (FEM). The electron effective mass of 0.24 m_0 [30] for ZnO and 0.35 m_0 [31] for MgO were used, and the band-offset value between the conduction band minimums of ZnO and MgO was taken as 3.59 eV following the result of x-ray photoelectron spectroscopy [17].

3. Results and discussion

Figure 2(a) presents the calculated electron energy levels and wave functions in a one-dimensional confined ZnO/MgO quantum well. The thickness of the ZnO well layer is 3 nm along the x direction. In such a quantum well, there are five bound states with energies of 0.13 eV, 0.51 eV, 1.14 eV, 2.02 eV and 3.08 eV corresponding to quantum numbers $n = 1, 2, 3, 4$ and 5, respectively. If combined with another confinement in y direction, the ZnO/MgO quantum well will have more bound states. The energy levels in the two-dimensional case are decided by the quantum numbers n_x and n_y [32]. According to their different characters, these bound states can be artificially divided into three distinct types: type-1 ($n_x \geqslant 1$ and $n_y = 1$), type-2 ($n_x = 1$ and $n_y > 1$) and type-3 ($n_x > 1$ and $n_y > 1$). Based on our calculations, we find that the energy seperations of type-1 and type-2 states are mainly decided by the well widths in the x and y directions, respectively. As

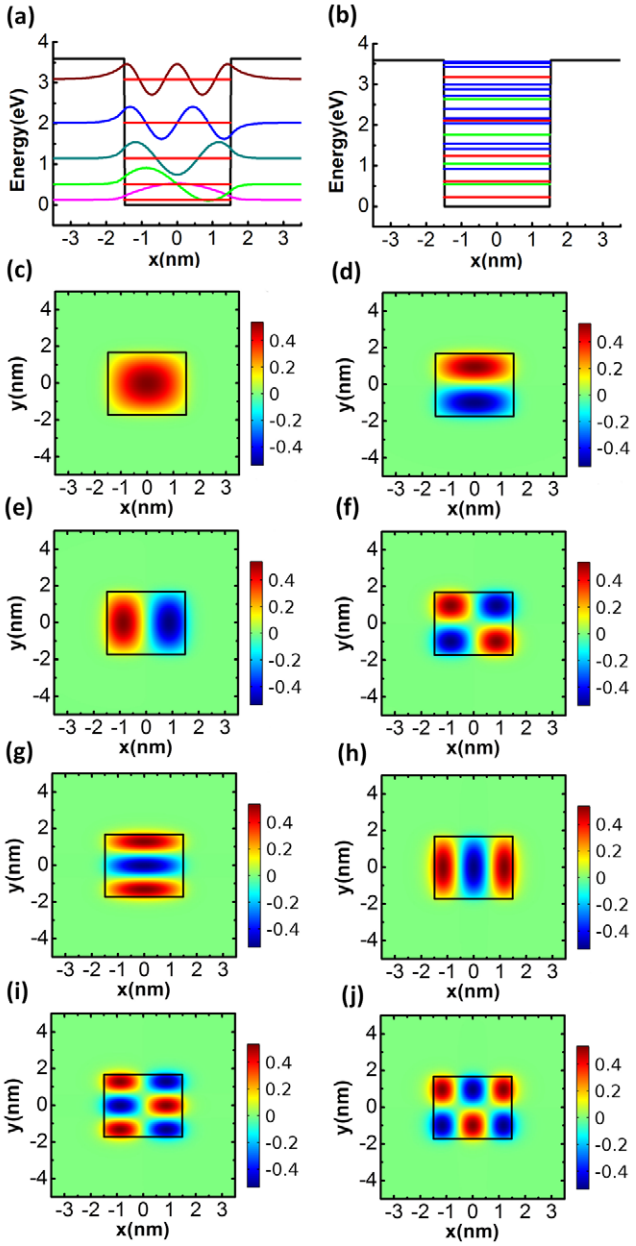

Figure 2. (a) Scheme of electron energy levels (red line) and wave functions(pink, green, dark green, blue and brown lines) in a one-dimensional ZnO/MgO quantum well(confined along x direction). The black line represents the conduction band profile of ZnO and MgO. (b) Scheme of electron levels in a two-dimensional ZnO/MgO quantum well(confined along both x and y directions). The red, green and blue lines correspond respectively to the type-1, type-2 and type-3 states. The electron wave function of the lowest eight energy levels are demonstrated from low to high as follows: (c) $|1,1\rangle$, (d) $|1,2\rangle$, (e) $|2,1\rangle$, (f) $|2,2\rangle$, (g) $|1,3\rangle$, (h) $|3,1\rangle$. (i) $|2,3\rangle$, (j) $|3,2\rangle$. The small rectangles in the center of the graphs stand for the boundary between ZnO and MgO, with ZnO within and MgO outside.

for type-3 states, the energy separations are decided by the well width in both x and y directions. It indicates that if the quantum cascade direction is along the x direction, the energy difference between a type-1 state and a type-2 state can be modulated close to the LO-phonon energy by controlling the width of the quantum well in the y direction. For example,

Table 1. New defined intersubband optical matrix element (in $\mathrm{nm}^{-1}\hbar^{-1}$) and dipole matrix elements (in nm).

Transition	$P'_{ij,x}(M_{ij,x})$	$P'_{ij,y}(M_{ij,y})$	Transition	$P'_{ij,x}(M_{ij,x})$	$P'_{ij,y}(M_{ij,y})$
$\|3,2\rangle \to \|2,3\rangle$	0(0)	0(0)	$\|3,1\rangle \to \|2,2\rangle$	0(0)	0(0)
$\|3,2\rangle \to \|3,1\rangle$	0(0)	−0.68(0.71)	$\|3,1\rangle \to \|2,1\rangle$	1.37(−0.69)	0(0)
$\|3,2\rangle \to \|1,3\rangle$	0(0)	0.001(0.003)	$\|3,1\rangle \to \|1,2\rangle$	0(0)	0(0)
$\|3,2\rangle \to \|2,2\rangle$	1.37(−0.69)	0(0)	$\|3,1\rangle \to \|1,1\rangle$	0(0)	0(0)
$\|3,2\rangle \to \|2,1\rangle$	0(0)	0(0)	$\|1,3\rangle \to \|2,2\rangle$	0(0)	0(0)
$\|3,2\rangle \to \|1,2\rangle$	0(0)	0(0)	$\|1,3\rangle \to \|2,1\rangle$	−0.001(0.001)	0(0)
$\|3,2\rangle \to \|1,1\rangle$	0(0)	0.001(0.001)	$\|1,3\rangle \to \|1,2\rangle$	0(0)	−1.23(0.76)
$\|2,3\rangle \to \|3,1\rangle$	−0.003(−0.003)	0(0)	$\|1,3\rangle \to \|1,1\rangle$	0(0)	0(0)
$\|2,3\rangle \to \|1,3\rangle$	0.76(−0.64)	0(0)	$\|2,2\rangle \to \|2,1\rangle$	0(0)	−0.68(0.71)
$\|2,3\rangle \to \|2,2\rangle$	0(0)	−1.23(0.77)	$\|2,2\rangle \to \|1,2\rangle$	0.76(−0.63)	0(0)
$\|2,3\rangle \to \|2,1\rangle$	0(0)	0(0)	$\|2,2\rangle \to \|1,1\rangle$	0(0)	0(0)
$\|2,3\rangle \to \|1,2\rangle$	0(0)	0(0)	$\|2,1\rangle \to \|1,2\rangle$	0(0)	0(0)
$\|2,3\rangle \to \|1,1\rangle$	0.001(0.001)	0(0)	$\|2,1\rangle \to \|1,1\rangle$	0.76(−0.63)	0(0)
$\|3,1\rangle \to \|1,3\rangle$	0(0)	0(0)	$\|1,2\rangle \to \|1,1\rangle$	0(0)	−0.68(0.70)

when the confinement along the y direction is 3.4 nm (whose energy levels and wave functions are shown respectively in figures 2(b)–(j)), the energy difference between $|1,2\rangle$ and $|2,1\rangle$ in this two-dimensional confined quantum well is about 74 meV, which approximates to the LO-phonon energy in ZnO. We also estimated the possibilities of optical transitions between the bound states in two-dimensional confined quantum wells. According to Fermi's golden rule, the probability of an optical stimulated transition [33] is:

$$\tilde{P}_{ij} = \frac{2\pi}{\hbar}|\langle\psi_i|V|\psi_j\rangle|\cdot\delta(\epsilon_f - \epsilon_i - \hbar\omega)\cdot f(\epsilon_i)[1 - f(\epsilon_j)] \quad (1)$$

where ϵ_i and ϵ_j are the energy of quantum states i and j, respectively, $\hbar\omega$ is the photon energy, and $f(\epsilon)$ represents the Fermi distribution. Here, $V = \frac{ieF}{2m_0\omega}\vec{\varepsilon}\cdot\vec{p}$, where F and $\vec{\varepsilon}$ are respectively the electric field amplitude and unit vector of the light wave. e and $\vec{p}$ are respectively the the electron charge and electron momentum. In the case of the two-dimensional quantum well as indicated by figure 2, the wave function of state i is given by:

$$\psi_i = \varphi_{\mathrm{Bl},i}(\vec{r})\varphi_{\mathrm{Env},i}(\vec{r}) \quad (2)$$

$$= \varphi_{\mathrm{Bl},i}(\vec{r})\frac{1}{\sqrt{L}}\mathrm{e}^{-\mathrm{i}kz}\phi_i(x,y) \quad (3)$$

Here $\varphi_{\mathrm{Bl},i}(\vec{r})$ is the Bloch function, $\phi_i(x,y)$ is the envelope function of the ith subband of the xy-confined quantum well, and L is the sample thickness in the z direction. The intersubband optical matrix element is:

$$P_{ij} = \langle\psi_i|\vec{\varepsilon}\cdot\vec{p}\,|\psi_j\rangle \quad (4)$$

$$\approx \vec{\varepsilon}\langle\varphi_{\mathrm{Bl},i}|\,\vec{p}\,|\varphi_{\mathrm{Bl},j}\rangle\langle\varphi_{\mathrm{Env},i}|\varphi_{\mathrm{Env},j}\rangle + \langle\varphi_{\mathrm{Bl},i}|\varphi_{\mathrm{Bl},j}\rangle\langle\varphi_{\mathrm{Env},i}|\vec{\varepsilon}\cdot\vec{p}\,|\varphi_{\mathrm{Env},j}\rangle \quad (5)$$

By definition the Bloch functions are identical for both subbands e.g. $\langle\varphi_{\mathrm{Bl},i}|\varphi_{\mathrm{Bl},j}\rangle = 1$ and $\langle\phi_{\mathrm{Bl},i}|\,\vec{p}\,|\phi_{\mathrm{Bl},j}\rangle = 0$, the intersubband optical matrix element becomes:

$$P_{ij} = \langle\varphi_{\mathrm{Env},i}|\vec{\varepsilon}\cdot\vec{p}\,|\varphi_{\mathrm{Env},j}\rangle \quad (6)$$

$$= \frac{1}{L}\int \mathrm{d}^3\vec{r}\,\mathrm{e}^{-\mathrm{i}kz}\phi_i(x,y)[e_x p_x + e_y p_y + e_z p_z]\mathrm{e}^{\mathrm{i}k'z}\phi_j(x,y) \quad (7)$$

The e_z term vanishes after integration, except if the initial and final states are identical($i = j$ and $k = k'$), thus the intersubband optical matrix element can be written as:

$$P'_{ij} = P'_{ij,x}e_x + P'_{ij,y}e_y \quad (8)$$

$$= \langle\phi_i(x,y)|\,p_x\,|\phi_j(x,y)\rangle e_x + \langle\phi_i(x,y)|\,p_y e_y|\phi_j(x,y)\rangle e_y, \quad (9)$$

where P'_{ij} is a new defined intersubband optical matrix element. With P'_{ij}, we can estimate the transition possibilities of bound states in the two-dimensional quantum wells, as shown in table 1. As a supplement, the dipole matrix elements $M_{ij} = \langle\phi_i(x,y)|\vec{r}|\phi_j(x,y)\rangle$ were also calculated. We find the selection rules for the intersubband optical transition of the two-dimensional confined quantum well scheme: 1. Optical transitions are forbidden to occur between type-1 states and type-2 states; 2. There is a higher chance for the optical transition to occur between the same type states on condition that the sum of quantum numbers differences $\triangle n_{ij} = n_i - n_j = (n_{ix} + n_{iy}) - (n_{jx} + n_{jy})$ is odd(type-1 states or type-2 states) or even(type-3 states), in agreement with the selection rule for the intersubband optical transitions of one-dimensional confined wells [34].

On the basis of the above optical transition rules, we designed a two-dimensional confined ZnO/MgO QCL with the well width $x = 3.8$ nm and length $y = 4.1$ nm as shown in figure 3(a). With a 123.0 KV cm^{-1} external electric field, the ground state $|1,1\rangle$ electrons in well 1 will resonantly tunnel to state $|3,1\rangle$ (labelled as E_4) in well 2. We find the energy differences between the E_4 level and any state in well 3 is lager than 120 meV, so that the electrons in state $|3,1\rangle$ will not tunnel into any higher state in well 3. Moreover, due to the large band offset of ZnO/MgO, the electrons in state $|3,1\rangle$ are tightly confined in the quantum well evidenced by the

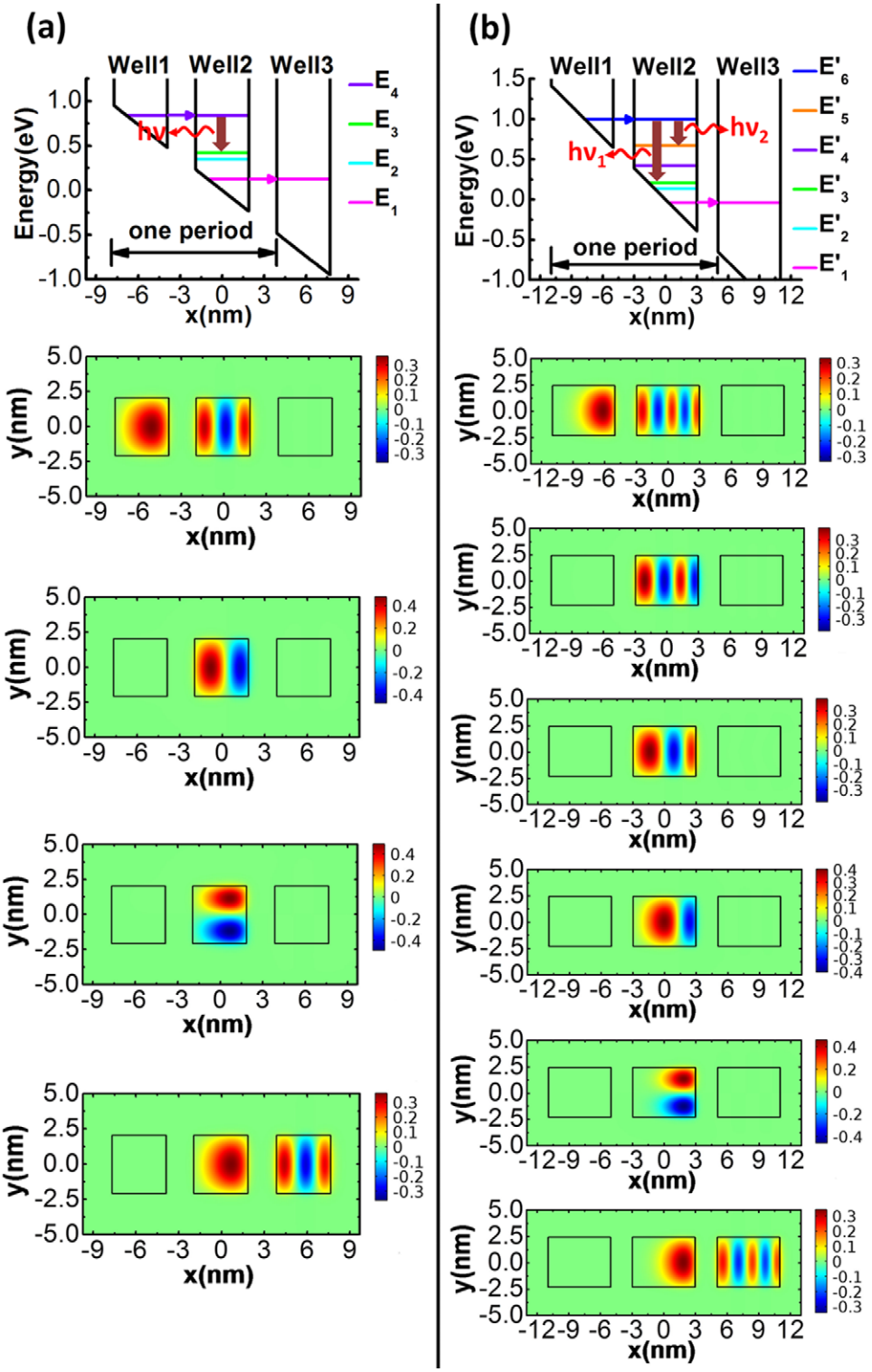

Figure 3. Schematic illustration of the photon emission process of the two-dimensional confined QCLs. (a) The topmost graph showed the relative optical transition energy levels in two-dimensional confined QCLs with the well widths x = 3.8 nm and $y = 4.1$ nm and 123.0 KV cm^{-1} external electric field. The rest graphs are the electrons wave functions from top to bottom corresponding to E_4, E_3, E_2 and E_1. (b) The relative optical transition energy levels and wave functions in two-dimensional confined QCLs with the well scale $x = 6$ nm, $y = 4.7$ nm and 129.3 KV cm^{-1} external electric field, the electrons wave functions from top to bottom corresponding to E'_6, E'_5, E'_4, E'_3, E'_2 and E'_1.

electron wave function distribution of E_4 level (the second graph from the top in figure 3(a)). Then, electrons in state $|3, 1\rangle$ will transit to state $|2, 1\rangle$ (labelled as E_3) with photon emissions of $h\nu = 0.42$ eV ($\approx$2.95 μm). Afterwards, electrons in state $|2, 1\rangle$ will decay rapidly to state $|1, 2\rangle$ (labelled as E_2) via the resonant LO-phonon emissions, since the energy difference between E_3 and E_2 is about 74 meV, fairly close to the LO-phonon energy in ZnO. On account that the electron–phonon scattering is extremely fast, the lifetime of $|2, 1\rangle$ could be very short, hence a large population inversion will be

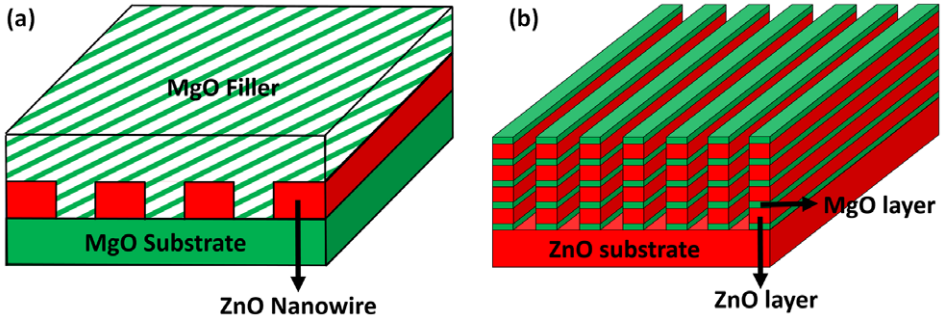

Figure 4. Schematic illustration of two ways to realize two-dimensional confined QCLs: (a) specific-size ZnO nanowires are put on a MgO substrate, then filling the intervals between ZnO nanowires by MgO epitaxial growth. (b) etching troughs on a ZnO/MgO superlattice.

established between $|3,1\rangle$ and $|2,1\rangle$. Afterwards the electrons in state $|1,2\rangle$ will jump down to the lowest-energy ground state $|1,1\rangle$ (labelled as E_1). And then the cascade processes will continuously occur in each pumped period of the QCL. It is notable that the calculated optical matrix elements of the transition from $|1,2\rangle$ to $|1,1\rangle$ is about 0.43 $(\text{nm}\cdot\hbar)^{-1}$, which is smaller than that from $|3,1\rangle$ to $|2,1\rangle$(about 0.73 $(\text{nm}\cdot\hbar)^{-1}$). This means the optical transition rate from $|1,2\rangle$ to $|1,1\rangle$ will be smaller than that from $|3,1\rangle$ to $|2,1\rangle$ at the beginning. As a result the electrons will accumulate in state $|1,2\rangle$. However, in our opinion the accumulation will not have a large influence on the population inversion. On one hand, according to equation (1) when the Fermi distribution of $|1,2\rangle$ reaches to a certain extent the optical transition rate from $|1,2\rangle$ to $|1,1\rangle$ will become larger than that from $|3,1\rangle$ to $|2,1\rangle$, so that state $|1,2\rangle$ will not be completely filled. On the other hand, based on Bastard's theory [35, 36], when the energy difference between the initial and final states is close to the LO-phonon energy, the electron–phonon scattering rate can be extremely large and does not depend much on the Fermi distribution of the initial and final states.

For producing shorter lasing wavelengths, we designed another two-dimensional confined QCL, as shown in figure 3(b). Its dimension is 6.0 nm in the x direction and 4.7 nm in the y direction. The lasing mechanism of this QCL is similar to the previous one. The difference lies in that, with the external electric field applied as 129.3 KV cm^{-1}, the electrons in the ground state in well 1 of this QCL will resonantly tunnel to a higher bound state—$|5,1\rangle$ (labelled as E_6') in well 2. Electrons in $|5,1\rangle$ have possibilities to transit to $|4,1\rangle$(labelled as E_5') or $|2,1\rangle$ (labelled as E_3') with photon emissions of $h\nu_2 = 0.32$ eV($\approx$3.82 μm) and $h\nu_1 = 0.79$ eV ($\approx$1.57 μm), respectively. The energy difference between $|2,1\rangle$ and $|1,2\rangle$ (labelled as E_2') is about 70 meV. If the well width in the x direction is reduced to 5 nm, the energy of photons generated by transitions from $|5,1\rangle$ to $|2,1\rangle$ will increase to 1.10 eV($\approx$1.13 μm). Meanwhile, the well width along the y direction should be reduced to 3.7 nm to adjust the energy difference between $|2,1\rangle$ and $|1,2\rangle$ to match the LO-phonon energy in ZnO. At this time, the external electric field should be adjusted to 203.8 KV cm^{-1}, making the ground state $|1,1\rangle$ in one well in full resonance with the upper state $|5,1\rangle$ in its adjacent well. With the purpose of producing even shorter lasing wavelengths, we designed another two-dimensional confined QCL with the well dimension of 6.2 nm $\times$ 3.4 nm. With a higher external electric field of 252.0 KV cm^{-1}, the ground state $|1,1\rangle$ electrons in one well could be injected into $|7,1\rangle$ of the adjacent well. Theoretically, QCLs with shorter wavelengths around 734 nm could be realized (through the transition from $|7,1\rangle$ to $|2,1\rangle$). It is worth mentioning that the higher the optical transition level used, the lower the emission efficiency of the two dimensional confined QCL would be. That is because the electrons in the higher energy levels have more possibility to jump to the undesired states, such as $|7,1\rangle$ to the states of $|6,1\rangle$ and $|4,1\rangle$.

While adding another dimensional confinement can not only expand the frequency range, but also increase the tunability of QCLs, it would be meaningful to use these QCLs in gas detection. For such applications, it would be favorable to design a laser operating at the frequency resonant with an infrared absorption line of a gas to be detected. However, in practice, it is not easy to tune the frequency of QCLs to resonate with a very narrow molecular absorption line, while maintaining the energy difference between the first excited state and ground state equal to the LO-phonon energy to create the population inversion(even in the mid- or far infrared region). With more controlling freedoms, two-dimensional confined QCLs may be able to satisfy both conditions: population inversion and resonance with the molecular absorption line in gas detection.

In practical experiments, we propose two ways to realize the two-dimensional confined QCLs. One way is to grow (or place) the uniform-sized ZnO nanowires on a MgO substrate in equal distance, then fill the intervals between those nanowires and cover them with epitaxially grown MgO as shown in figure 4(a). However, nowadays, it still seems challenging to control the size of ZnO nanowires precisely according to the accuracy required by the two-dimensional confined QCLs. The other way is to grow ZnO and MgO thin films one on another to form a superlattice in the first place, then troughs are etched chemically or by electron beam on a ZnO/MgO superlattice as shown in figure 4(b). The quantum confinement in the other direction is only determined by the distance between the troughs. For now, the etching precision would be another key problem of controlling such short distances between the troughs in the fabrication processes. But with the development of a processing technique, it would only be a matter of time for such two-dimensional confined QCLs to

be realized successfully with much shorter lasing wavelengths than before.

4. Conclusion

In conclusion, we demonstrate theoretically that two-dimensional confined QCLs can be used to extend the spectral range of QCLs to a much higher frequency region. Based on FEM calculation results, we show that the two-dimensional confined ZnO/MgO QCLs can produce lasing with wavelengths at $\lambda = 2.95\ \mu$m, 1.57 μm, 1.13 μm and 734 nm. The emission wavelength could be tuned by controlling the external electric field and well size. This strategy to design QCLs may pave a new way to fabricate semiconductor lasers in the near future.

Acknowledgments

This work is supported by the National Basic Research Program of China (973 Program No. 2011CB302006 and No. 2011CB302005), the National Science Fund for Distinguished Young Scholars (No. 61525404), the National Natural Science Foundation of China (No. 11174273, No. 11134009 and No. 61306054), and the 100 Talents Program of the Chinese Academy of Sciences.

References

[1] Faist J, Capasso F, Sivco D L, Sirtori C, Hutchinson A L and Cho A Y 1994 *Science* **264** 553
[2] Cathabard O, Teissier R, Devenson J, Moreno J C and Baranov A N 2010 *Appl. Phys. Lett.* **96** 141110
[3] Devenson J, Teissier R, Cathabard O and Baranov A N 2007 *Appl. Phys. Lett.* **90** 111118
[4] Devenson J, Teissier R, Cathabard O and Baranov A N 2007 *Appl. Phys. Lett.* **91** 251102
[5] Ohtani K and Ohno H 2003 *Appl. Phys. Lett.* **82** 1003
[6] Nobile M, Klang P, Mujagić E, Detz H, Andrews A, Schrenk W and Strasser G 2009 *Electron. Lett.* **45** 1031
[7] Yao Y, Hoffman A J and Gmachl C F 2012 *Nat. Photon.* **6** 432
[8] Williams B S 2007 *Nat. Photon.* **1** 517
[9] Deutsch C *et al* 2010 *Appl. Phys. Lett.* **97** 261110
[10] Scalari G, Turcinková D, Lloyd-Hughes J, Amanti M I, Fischer M, Beck M and Faist J 2010 *Appl. Phys. Lett.* **97** 081110
[11] Apalkov V and Stockman M I 2014 *Light: Sci. Appl.* **3** e191
[12] Faist J, Capasso F, Sivco D L, Hutchinson A L, Chu S-N G and Cho A Y 1998 *Appl. Phys. Lett.* **72** 680
[13] Devenson J, Barate D, Cathabard O, Teissier R and Baranov A N 2006 *Appl. Phys. Lett.* **89** 191115
[14] Revin D G, Cockburn J W, Steer M J, Airey R J, Hopkinson M, Krysa A B, Wilson L R and Menzel S 2007 *Appl. Phys. Lett.* **90** 021108
[15] Semtsiv M P, Wienold M, Dressler S and Masselink W T 2007 *Appl. Phys. Lett.* **90** 051111
[16] Keck I, Schmult S, Wegscheider W, Rother M and Mayer A P 2003 *Phys. Rev.* B **67** 125312
[17] Li Y F *et al* 2008 *Appl. Phys. Lett.* **92** 192116
[18] Shi K, Zhang P F, Wei H Y, Ziao C M, Li C M, Liu X L, Yang S Y, Zhu Q S and Wang Z G 2012 *Solid State Commun.* **152** 938
[19] Janotti A and Van de Walle C G 2007 *Phys. Rev.* B **75** 121201
[20] Betancourt J, Saavedra-Arias J J, Burton J D, Ishikawa Y, Tsymbal E Y and Velev J P 2013 *Phys. Rev.* B **88** 085418
[21] Teke A, Özgür Ü, Doğan S, Gu X and Morkoc H 2004 *Phys. Rev.* B **70** 195207
[22] Pan X H, Guo W, Ye Z Z, Liu B, Che Y, He H P and Pan X Q 2009 *J. Appl. Phys.* **105** 113516
[23] Zhang H Q, Hu L Z, Zhao Z W, Ma J X, Qiu Y, Wang B, Liang H W and Bian J M 2011 *Vacuum* **85** 718
[24] Bellotti E, Driscoll K, Moustakas T D and Paiella R 2008 *Appl. Phys. Lett.* **92** 101112
[25] Williams B S, Kumar S, Qin Q, Hu Q and Reno J L 2006 *Appl. Phys. Lett.* **88** 261101
[26] Wang Q J, Pflügl C, Diehl L, Capasso F, Edamura T, Furuta S, Yamanishi M and Kan H 2009 *Appl. Phys. Lett.* **94** 011103
[27] Bai Y, Slivken S, Kuboya S, Darvish S R and Rageghi M 2010 *Nat. Photon.* **4** 99–102
[28] Liu H C 2010 *Nat. Photon.* **4** 69–70
[29] Kolek A, Hałaś G and Bugajski M 2012 *Appl. Phys. Lett.* **101** 061110
[30] Baer W S 1967 *Phys. Rev.* B **154** 785
[31] Xu Y N and Ching W Y 1991 *Phys. Rev.* B **43** 4461
[32] Harrison P 2005 *Quantum Wells, Wires and Dots: Theoretical and Computational Physics* 2nd edn (Chichester: Wiley) pp 248–54
[33] Helm M 2000 *Intersubband Transitions in Quantum Wells: Physics and Device Applications I* (*Semiconductors and Semimetals* vol 62) ed H C Liu and F Capasso (San Diego: Academic) chapter 1 pp 1–99
[34] Yang R Q 1995 *Phys. Rev.* B **52** 11958
[35] Ferreira R and Bastard G 1989 *Phys. Rev.* B **40** 1074
[36] Bockelmann U and Bastard G 1990 *Phys. Rev.* B **42** 8947